Published in final edited form as:
Br J Haematol. 2013 April ; 161(1): 43–56. doi:10.1111/bjh.12206.

THE BTK INHIBITOR PCI-32765 SYNERGISTICALLY INCREASES PROTEASOME INHIBITOR ACTIVITY IN DLBCL AND MCL CELLS SENSITIVE OR RESISTANT TO BORTEZOMIB

Girija Dasmahapatra[1], **Hiral Patel**[1], **Paul Dent**[2,3,4], **Richard I. Fisher**[6], **Jonathan Friedberg**[6], and **Steven Grant**[1,3,4,5,¶]

[1]Division of Hematology/Oncology, Department of Medicine, Virginia Commonwealth University, Richmond VA

[2]Department of Neurosurgery, Virginia Commonwealth University, Richmond VA

[3]Department of Biochemistry, Virginia Commonwealth University, Richmond VA

[4]Department of Molecular and Human Genetics, Virginia Commonwealth University, Richmond VA

[5]Massey Cancer Center, Virginia Commonwealth University, Richmond VA

[6]Division of Hematology Oncology, University of Rochester Medical Center and the James T. Wilmot Cancer Center, Rochester, N.Y.

Summary

Interactions between the Bruton tyrosine kinase (BTK) inhibitor PCI-32765 and the proteasome inhibitor (bortezomib) were examined in diffuse large-B cell lymphoma (DLBCL) and mantle cell lymphoma (MCL) cells, including those highly resistant to bortezomib. Co-administration of PCI-32765/bortezomib synergistically increased mitochondrial injury and apoptosis in germinal centre- or activated B-cell-like-DLBCL cells and in MCL cells. These events were accompanied by marked AKT and nuclear factor (NF)-κB (NFKB1) inactivation, down-regulation of Mcl-1 (MCL1), Bcl-xL (BCL2L1), and XIAP, and enhanced DNA damage (e.g., γH2A.X formation) and endoplasmic reticulum (ER) stress. Similar interactions were observed in highly bortezomib-resistant DLBCL and MCL cells, and in primary DLBCL cells. In contrast, PCI-32765/bortezomib regimens displayed minimal toxicity toward normal $CD34^+$ bone marrow cells. Transfection of DLBCL cells with a constitutively active AKT construct attenuated AKT inactivation and significantly diminished cell death, whereas expression of an NF-κB "super-repressor" ($I\kappa B\alpha_{ser34/36}$) increased both PCI-32765 and bortezomib lethality. Moreover, cells in which the ER stress response was disabled by a dominant-negative eIF2α construct were resistant to this regimen. Finally, combined exposure to PCI-32765 and bortezomib resulted in more pronounced

¶To whom reprint requests should be sent as follows: Division of Hematology/Oncology, Virginia Commonwealth University Room 234, Goodwin Research Building 401 College Street Richmond VA 23298 Tel: +1 804-828-5211 Fax: +1 804-828-8079 stgrant@vcu.edu.

Disclosure: None

Competing interest: the authors have no competing interests

Author contributions: Girija Dasmahapatra - designed the research study, performed the research, acquired and analysed the data, helped to write the paper
Hiral Patel - designed the research study, performed the research, acquired and analysed the data
Paul Dent – helped to design the research study, analysed the data, critically reviewed and helped to write the paper
Richard I. Fisher – helped to design the research study, critically reviewed and helped to write the paper
Jonathan Friedberg - helped to design the research study, critically reviewed and helped to write the paper
Steven Grant- designed the research study, supervised the research study, interpreted the data, and wrote the paper

and sustained reactive oxygen species (ROS) generation, and ROS scavengers significantly diminished lethality. Given promising early clinical results for PCI-32765 in DLBCL and MCL, a strategy combining BTK/ proteasome inhibitor warrants attention in these malignancies.

Keywords

PCI32765; bortezomib; BTK; DLBCL; mantle cell lymphoma

INTRODUCTION

The Bruton tyrosine kinase (BTK) is a member of the TEC family of tyrosine kinases and is involved in B-cell antigen receptor (BCR) signalling (Hussain *et al*, 2011). Chronic BTK activation has been implicated in the pathogenesis of certain B-cell malignancies (Davis *et al*, 2010). BCR activation leads to BTK plasma membrane translocation, phosphorylation at Y_{551} by members of the Src family kinases (e.g., BLK, LYN, FYN, and SYK), and autophosphorylation at Y_{223} (Rawlings *et al*, 1996). BTK induction then triggers activation of phospholipase C and Ca^{+2} mobilization, leading in turn to downstream events (e.g., proliferation, differentiation) mediated through multiple transcription factors (e.g, nuclear factor [NF]-κB (NFKB1], NF-AT) and survival signalling cascades e.g., Ras/Raf/MEK/ ERK and PI3K/AKT (Mohamed *et al*, 2009).

PCI-32765 (Ibrutinib) is a selective and irreversible BTK inhibitor that binds covalently to a Cys_{481} residue with the BTK active site, preventing Tyr_{223} phosphorylation required for activation (Honigberg *et al*, 2010). Preclinical studies in chronic lymphocytic leukaemia (CLL) demonstrated inhibition of proliferation and/or induction of cell death by PCI-32765, associated with interruption of three signalling pathways critical for malignant B cell survival (Lopez-Guerra & Colomer, 2010;Wickremasinghe *et al*, 2011;Castillo *et al*, 2012) e.g. NF-κB, ERK1/2, and AKT (Herman *et al*, 2011). Importantly, PCI-32765 has shown significant activity in refractory/relapsed CLL/small lymphocytic leukaemia (SLL) (O'Brien *et al*, 2011; Harrison, 2012).

Diffuse large-B-cell lymphoma (DLBCL), an aggressive form of non-Hodgkin lymphoma (NHL), has been divided into three groups based upon gene profiling patterns: germinal-centre B-cell-like DLBCL (GC-DLBCL), activated B-cell-like DLBCL (ABC-DLBCL) and mediastinal or unclassified type (Staudt & Dave, 2005). These sub-categories exhibit distinct differences in survival, chemo-responsiveness, and NF-κB status (Bea *et al*, 2005). For example, ABC-DLBCL is associated with activation of and dependence upon NF-κB regulatory genes (e.g., *TNFAIP3, CARD11*) (Compagno *et al*, 2009), and has a significantly worse prognosis than other sub-types (Bea *et al*, 2005). Mantle cell lymphoma (MCL) is associated with short disease-free and overall survivals characteristic of aggressive lymphomas (Williams *et al*, 2011). Recently, BTK has been shown to be critical for BCR signalling and survival of ABC-DLBCL cells expressing wild-type CARD11, an NF-κB adaptor protein, but not for cells with mutant CARD11 or GC-DLBCL (Davis *et al*, 2010). Furthermore, ibrutinib displays significant preclinical activity against ABC-DLBCL cells *in vitro* and *in vivo* (Balbasubramanian *et al*, 2011), and encouraging activity in relapsed/ refractory ABC-DLBCL (Harrison, 2012;Staudt *et al*, 2011). Initial phase II trials results in patients with relapsed/refractory disease also appear promising (Wang *et al*, 2011).

The ubiquitin-proteasome system degrades diverse intracellular proteins, and plays an important role in responses to cellular stresses (oxidative injury and DNA damage), maintenance of the balance between pro- and anti-apoptotic proteins, and signal transduction regulation (Bedford *et al*, 2011). The boronic anhydride, bortezomib, a reversible

proteasome inhibitor, was the first to enter the clinic (Adams *et al*, 1999), and was approved for refractory multiple myeloma (Richardson *et al*, 2006). Bortezomib preferentially targets malignant cells and circumvents Bcl-2 (BCL2)-related resistance (An *et al*, 1998). Mechanisms of proteasome inhibitor lethality include accumulation of misfolded proteins and endoplasmic reticulum (ER) stress induction, oxidative injury, inhibition of NF-κB (by accumulation of IκBα), up-regulation of pro-apoptotic proteins (e.g., Bim [BCL2L11]), p53 (TP53) and JNK (MAPK8) stabilization, and interference with DNA repair (Nencioni *et al*, 2007). While PIs classically inhibit NF-κB, recent evidence indicates up-regulation in some cell types (Hideshima *et al*, 2009), including DLBCL, due to autophagic IκBα degradation (Jia *et al*, 2012). Bortezomib was approved for refractory MCL (Fisher *et al*, 2006); in contrast, it has limited single-agent activity in relapsed DLBCL (Goy *et al*, 2005). However, bortezomib significantly improved survival was observed in ABC-DLBCL (but not GC-) patients receiving dose-adjusted EPOCH (etoposide, doxorubicin, vincristine, prednisone, cyclophosphamide) (Dunleavy *et al*, 2009).

Several considerations support a strategy combining ibrutinib with proteasome inhibitors in NHL. First, in malignant B-cells, ibrutinib interrupts three pathways (e.g., NF-κB, AKT, and ERK1/2) (Herman *et al*, 2011) important for NHL cell survival (Lopez-Guerra & Colomer, 2010;Wickremasinghe *et al*, 2011;Castillo *et al*, 2012). Second, interruption of each of these pathways potentiates proteasome inhibitor lethality in malignant cells (Dai *et al*, 2003;Orlowski *et al*, 2002;Ikeda *et al*, 2010;Yeramian *et al*, 2012;Dasmahapatra *et al*, 2010;Dasmahapatra *et al*, 2012;Dasmahapatra *et al*, 2011). The present results demonstrate synergistic interactions between ibrutinib and bortezomib in bortezomib-sensitive or -resistant DLBCL and MCL cells, and support further pursuit of this strategy.

METHODS

Cells

SUDHL16, SUDHL6, SUDHL4 (all GC-subtype), OCI-LY10 (ABC-subtype) and Granta519, Rec-1 (both mantle cell) were obtained as described (Dasmahapatra *et al*, 2010;Dasmahapatra *et al*, 2011). Bortezomib-resistant SUDHL6-25BR (GC-DLBCL), OCI-LY10-40BR (ABC-DLBCL), Granta-25BR (haem) lines were generated as previously described (Dasmahapatra *et al*, 2010;Dasmahapatra *et al*, 2011). Cells ectopically expressing constitutively activated AKT were generated by transfecting pUSE-myr-AKT1 cDNA (Upstate Biotechnology, Lake Placid, NY) into SUDHL16 cells by electroporation as previously described (Dasmahapatra *et al*, 2012). Stable clones were selected by serial dilution using antibiotics. SUDHL16 cells were stably transfected with Ser32/Ser36-mutated IκBα cDNA (IκBα-SR) or an empty vector (pcDNA3.1) as described earlier (Dai *et al*, 2005). Stable clones expressing eIF2α–DN in SUDHL16 cells were generated using standard techniques as previously described (Rahmani *et al*, 2007;Dasmahapatra *et al*, 2009). All experiments were performed with logarithmically growing cells (e.g., 4.0 - 5.0 × 10^5 cells/ml). Mycoplasma tests were uniformly negative (MycoAlert Mycoplasma Detection Kit, Lonza, Inc., Rockland, ME, USA).

Reagents

Bortezomib (Velcade®) was provided by Millennium Pharmaceuticals (Cambridge, MA, USA). PCI-32765 was purchased from ChemieTek Inc. (Indianapolis, IN, USA). 7-Aminoactinomycin D (7-AAD), AKTi (inhibitor VIII) were purchased from Calbiochem, (Millipore, Billerica, MA, USA), Perifosine was provided by the National Cancer Institute Cancer Therapy Evaluation Program (Rockville, MD, USA). All agents were formulated in dimethyl sulfoxide (DMSO).

Experimental Format

Cells were cultured as previously described (Dasmahapatra *et al*, 2010). Cells were treated with desired drugs and prepared for analysis as described below.

Assessment of cell death and apoptosis

Cell viability was monitored by flow cytometry using 7-AAD staining as previously described (Dasmahapatra *et al*, 2010). Alternatively, Annexin V/propidium iodide (PI) staining (both BD PharMingen, San Diego, CA, USA) was employed to monitor early (Annexin V^+) or late (Annexin V^+, PI^+) apoptosis. In all studies, results of 7-AAD and Annexin V/PI assays were concordant.

Isolation of primary DLBCL mononuclear cells and $CD34^+$ cells

These studies have been approved by the Investigational Review Board of Virginia Commonwealth University. Primary DLBCL mononuclear cells (96% purity) were isolated by standard Ficoll-Hypaque separation; normal $CD34^+$ cells were isolated using an immunomagnetic bead separation technique, both as previously described (Dasmahapatra *et al*, 2010).

Western blot Analysis

Western blot samples were prepared from whole cell pellets as described (Dasmahapatra *et al*, 2010). Primary antibodies were sourced as follows: cytochrome C, phosphorylated (p)-FKHR, FKHR, 4EBP1, Mcl-1, p-eiF2α, eiF2α were from Santa Cruz Biotechnology (Santa Cruz, CA, USA); pAKT, AKT1, p-ERK, ERK, p-GSK3α/β, GSK3α/β, p-4EBP1, Bcl-xL, cleaved caspase-3 were from Cell Signaling Technology, Beverly, MA; SMAC was from Upstate Biotechnology; Tubulin and PARP were from Oncogene (San Diego, CA, USA). XIAP and Caspase-2 antibodies were purchased from BD BioScience (Sparks, MD, USA). γH2A.X was from Millipore.

Measurement of reactive oxygen species (ROS) Production

Cells were treated with 20 μM 2/,7/- dicholorodihydrofluorescein diacetate for 30 min at 37°C and fluorescence was monitored by flow cytometry using fluorescence-activated cell sorting (FACS) and analysed with Cell Quest software (Dasmahapatra *et al*, 2011).

NF-κB Activity

Nuclear protein was extracted using a Nuclear Extract Kit (Active Motif, Carlsbad, CA, USA). NF-κB activity was determined by enzyme-linked immunosorbent assay (ELISA) TransAM NF-κB p65 Transcription Factor Assay Kit (Active Motif), according to the manufacturer's instruction (Dasmahapatra *et al*, 2010;Dasmahapatra *et al*, 2011).

Electrophoretic mobility shift assay (EMSA)

Consensus oligonucleotides corresponding to the sites of the immunoglobulin κlight-chain enhancer binding for NF-κB were purchased from Promega (Madison, WI, USA) and labelled with [γ-^{32}P] ATP. Nuclear extracts were prepared by using NE-PER™ nuclear and cytoplasmic extraction reagents as described above. A total of 5 μg/condition of nuclear proteins was subjected to EMSA for NF-κB/DNA binding as described previously (Dasmahapatra *et al*, 2010;Dasmahapatra *et al*, 2011).

Terminal deoxynucleotidyl transferase dUTP nick end labelling (TUNEL) Assays

Slides were prepared by using 50-100 μl sample aliquots by cytospin. TUNEL assays were performed with fluorescein −12-dUTP using a terminal transferase recombinant kit (Roche,

Indianapolis, IN, USA; catalogue no 1373 242 & 220582 kit) and Vectashield / PI kit (Vectashield, Burlingame, CA, USA; catalogue no H-1200) as per the manufacturer's protocol (Dasmahapatra *et al*, 2012).

Wright Giemsa Staining

Slides were prepared similarly to the TUNEL assay and staining was done with a commercially available Diff-Quik stain kit (Dade-Behring, Newark, DE, USA) as per manufacturer's instruction.

Statistical Analysis

Differences between experimental conditions were assessed using two-sided 0.05 level *t*-tests. Synergistic drug interactions were formally tested by Median Dose Effect analysis in conjunction with a commercially available software program (CalcuSyn, Biosoft, Ferguson, MO) (Chou & Talalay, 1984).

RESULTS

PCI-32765 and bortezomib interact synergistically in ABC or GC DLBCL cells and MCL cells

Exposure (48 h) of GC- (SUDHL-4 or -6,-16) or ABC- (OCI-LY10) DLBCL cells to minimally toxic concentrations of bortezomib (e.g., 2.5 to 8 nM) or PCI-32765 (5 – 7.5 μM) in combination resulted in marked increases in cell death (Fig 1A). TUNEL assays (SUDHL6 cells) confirmed the pronounced increase in positivity with combined treatment (Supporting Fig 1A), while photomicrographs of Wright-Geimsa-stained specimens demonstrated the accompanying striking reduction in cells (Supporting Fig 1B). Very similar results were obtained in MCL cells (GRANTA519 and Rec1; Fig 1B). Moreover, significant potentiation of apoptosis was observed in each cell type over a range of concentrations of both bortezomib (e.g., SUDHL16; 1.5 – 4 nM, SUDHL4; 4-8 nM, SUDHL6; 2-6 nM, OCI-LY10; 4-8 nM) and PCI-32765 (e.g., SUDHL16 ; 3-5 μM, SUDHL4; 4-8 μM, SUDHL6; 3-8 μM, OCI-LY10; 5-10 μM), compared to single agent treatment (data not shown). Median Dose Effect analysis of cell death induction in SUDHL6 cells for constant ratios (1:2500) of bortezomib and PCI32765 yielded Combination Index (CI) values considerably less than 1.0, indicating a synergistic interaction (Fig 1C). Equivalent results (e.g., CI values ranging from 0.3 to 0.5) were obtained in multiple other cell types including SUDHL16, SUDHL4, OCI-LY10, Granta 519, and Rec-1 (data not shown). Time course analysis of cell death in SUDHL6 cells revealed clear increases in cell death for the combination after 24 h exposure, which became more pronounced over the ensuing 24 h (Fig 1D). Dose-response studies revealed that 48-h exposure of cells to 3 nM bortezomib in combination with 4 μM PCI-32765 resulted in significant increases in cell death, with further increases in apoptosis as the PCI32765 concentration was raised (Fig 1E). Finally, equivalent concentrations of bortezomib and PCI-32765 exposure (48 h) resulted in significantly enhanced cell death in primary DLBCL cells (GC subtype), but exerted little toxicity toward normal bone marrow $CD34^+$ cells (Fig 1F).

Co-exposure of DLBCL or MCL cells to PCI-32765 and bortezomib leads to enhanced mitochondrial injury and caspase activation, AKT pathway inactivation, down-regulation of anti-apoptotic proteins, DNA damage, and ER stress

The impact of combined exposure to PCI-32765 and bortezomib was then examined in DLBCL and MCL cells. These studies were performed at 24 h i.e., prior to the onset of extensive apoptosis, to reduce the confounding effects of cell death induction. Combined treatment of SUDHL6 cells with PCI-32765 and bortezomib resulted in a marked increase in

cytochrome c and SMAC release, accompanied by caspase-3 cleavage and PARP degradation (Fig 2A). Moreover, PCI-32765, particularly when combined with bortezomib, induced marked down-regulation of phospho-AKT and multiple downstream targets (e.g. GSK3, FHKR and 4EBP1 (Fig 2A). In contrast, little dephosphorylation of ERK1/2 was observed at this interval.

Combined treatment also resulted in a sharp reduction in the expression of several anti-apoptotic Bcl-2 family members, including Mcl-1 (MCL1), XIAP, and Bcl-xL (BCL2L1), as well as a clear increase in expression of γH2A.X, a marker of double-strand DNA breaks (Celeste *et al*, 2002) (Fig 2B). Finally, while individual treatment had only modest effects, combined exposure resulted in cleavage of caspase-2 expression accompanied by phosphorylation of eIF2α, indicators of ER stress induction (Teske *et al*, 2011).

Similar results were observed in ABCDLBCL (OCI-LY10) and MCL (Granta 519) cells, i.e., combined exposure resulted in clear increases in mitochondrial injury and caspase activation, more pronounced inactivation of AKT and down-regulation of anti-apoptotic proteins (e.g., Mcl-1), accompanied by increased expression of DNA damage/ γH2A.X, and evidence of ER stress (e.g. caspase-2 cleavage, eIF2α phosphorylation (Fig 2C and 2D). As observed in the case of SUDHL6 cells, OCI-LY10 cells failed to display ERK1/2 dephosphorylation with combined treatment, although moderate reductions were noted in Granta cells.

PCI-32765 and bortezomib interact synergistically in bortezomib-resistant DLBCL and MCL cells

Parallel studies were performed in DLBCL and MCL cells resistant to bortezomib. Exposure (48 h) to 15, 25, or 15 nM bortezomib, respectively, killed essentially 100% of parental SUDHL6, OCI-LY10, or Granta cells, but exerted only minimal toxicity toward their bortezomib-resistant counterparts (Fig 3A). However, co-administration of PCI-32765 at concentrations that were only modestly toxic by themselves to bortezomib-resistant cells (e.g. 6 to 7.5 μM) resulted in very pronounced cell death in each of the resistant cell lines (Fig 3B). Findings in bortezomib-resistant SUDHL6 cells were confirmed by TUNEL assays (Supporting Fig 2A) and examination of Wright-Geimsa-stained slides (Supporting Fig 2B). As observed in parental cells, combined exposure (24 h) of resistant SUDHL6 cells to PCI-32765 and bortezomib resulted in marked increases mitochondrial damage and caspase activation, as well as inactivation of the AKT pathway (Fig 3C). Co-treatment also resulted in down-regulation of anti-apoptotic proteins, enhanced DNA damage (γH2A.X formation), and evidence of ER stress (e.g. caspase-2 cleavage, eIF2α phosphorylation (Fig 3D). Similar results were obtained in other resistant lines (data not shown). Together, these findings indicate that the PCI-32765/bortezomib regimen is effective against bortezomib-resistant as well as -sensitive DLBCL and MCL cells and elicits similar changes in survival- and stress-related proteins.

AKT inactivation plays a significant functional role in PCI-32765/bortezomib synergism

To assess the functional significance of AKT inactivation in the activity of this regimen, SUDHL16 cells expressing a constitutively active (myristolated) form of AKT were employed as before (Dasmahapatra *et al*, 2012). Two clones (SUDHL16 CA-AKT Cl 2 and Cl 6) expressed clear increases in phospho-AKT and GSK-3α/β compared to empty vector controls (Fig 4A, inset). These clones were significantly more resistant to PCI-32765/ bortezomib-mediated cell death than controls ($P < 0.02$; Fig 4A). Consistent with these findings, cells expressing constitutively active AKT expressed higher levels of phospho-AKT, and displayed diminished levels of cleaved caspase-3, PARP, and γH2A.X compared to controls following combined bortezomib/PCI32765 (24 h) exposure (Fig 4B). Moreover,

the small molecule AKT inhibitor, perifosine, or the commercially available AKT inhibitor, AKTi, significantly potentiated bortezomib lethality relative to bortezomib treatment alone in SUDHL6 cells (Figure 4C). On the other hand, little change in p-ERK was observed in mutant or empty-vector controls with combined treatment. In separate studies, ectopic expression of constitutively active MEK1/2 did not significantly diminish bortezomib/PCI32765 activity (data not shown), arguing against the likelihood that ERK1/2 inactivation plays a significant role in the activity of this regimen. Together, these findings argue that inactivation of AKT contributes functionally to the activity of the PCI-32765/bortezomib regimen

Evidence for the contribution of NF-κB inactivation to PCI-32765/bortezomib synergism

The effects of combining PCI-32765 and bortezomib on NF-κB activation was then assessed in SUDHL6 and OCI-LY10 cells. EMSA analysis revealed that exposure (24 h) of cells to minimally toxic concentrations of PCI-32765 (6-7.5 μM) or bortezomib (3-8 nM) individually resulted in reductions in DNA binding activity (Fig 5A). Quantification of NF-κB activation by ELISA assay revealed that NF-κB activity after combined exposure to both agents was significantly less than activity in cells exposed to only one agent for both GC- (SUDHL6) as well as ABC- (OCI-LY10) DLBCL cells ($P < 0.05$; Fig 5B). To assess the functional significance of this phenomenon, parallel studies were performed with cells expressing an IκBα "super-repressor" construct. This construct, which cannot be phosphorylated by IKK on serine residues 34 and 36, is resistant to degradation, and thus binds to prevents translocation of p65 RelA to the nucleus, preventing its activation (Dai *et al*, 2005). Notably, super-repressor clones were significantly more sensitive to cell death induced by both PCI-32765 and bortezomib than their control counterparts ($P < 0.05$; Fig 5C) arguing that enhanced NF-κB inactivation following combined treatment contributes to PCI-32765/bortezomib actions. Finally, the effects of combined treatment with PCI32765 and bortezomib were examined in SUDHL6-26BR cells. Combined treatment with PCI-32765 and bortezomib significantly enhanced inhibition of NF-kB compared to single-agent treatment in these bortezomib-resistant cells, as observed in their sensitive counterparts (Figure 5D).

Role of the ER stress response in PCI-32765/bortezomib activity in DLBCL cells

The preceding findings indicated that combined exposure of bortezomib-sensitive or -resistant DLBCL cells to PCI-32765 and bortezomib resulted in evidence of ER stress, manifested by cleavage of capases-2, and phosphorylation of eIF2α, a component of the unfolded protein response responsible for blocking protein translation (Xu *et al*, 2005). To determine whether this phenomenon contributed to apoptosis, effects of the PCI-32765/bortezomib regimen were compared in empty-vector control SUDHL16 cells versus cells expressing a dominant-negative form of eIF2α (Rahmani *et al*, 2007). As shown in Fig 6A, two clones (eIF2α-DN Cl16 and Cl24) were significantly more resistant to PCI-32765/bortezomib-induced cell death than controls ($P <0.05$). Consistent with these results, cells expressing DN clones displayed reduced caspase-3 degradation and PARP cleavage compared to controls, although inactivation of AKT was equivalent (Fig 6B). These findings suggest that the ER stress response contributes to PCI-32765/bortezomib anti-lymphoma effects, and argue that this phenomenon operates downstream of AKT inactivation. In contrast, expression of dominant-negative eIF2α partially but clearly inhibited the induction of DNA damage reflected by γH2A.X formation.

Combined exposure to PCI-32765 and bortezomib leads to oxidative injury-mediated cell death in DLBCL cells

Previous studies by our group (Yu *et al*, 2004) and others (Ling *et al*, 2003) have linked bortezomib-mediated activity to oxidative injury (e.g. ROS generation). To determine

whether this phenomenon might contribute to PCI-32765/bortezomib interactions, ROS generation was monitored in OCI-LY10 cells following exposure to the agents individually and in combination. Exposure to bortezomib (8 nM) resulted in an increase in ROS at 10 h, which increased gradually over the ensuing 24 h (Fig 7A). Interestingly, exposure to PCI-32765(6.0μM) alone led to a clear increase in ROS after 1 h, which began to decline by 4 h, and returned to baseline levels by 18 h. To the best of our knowledge, this is the first demonstration that PCI-32765 induces, albeit transiently, ROS in transformed cells. Notably, combined exposure to PCI-32765 and bortezomib induced ROS at early intervals, as in the case of PCI-32765 alone, but in contrast, levels increased over the entire 36-h exposure interval. Thus, combining PCI-32765 with bortezomib resulted in both more sustained as well as pronounced ROS generation. To assess the functional significance of this phenomenon, cells were co-incubated with the ROS scavenger TBAP. Co-administration of TBAP significantly reduced ROS induced by bortezomib or the PCI-32765/bortezomib regimen (Fig 7B), and partially but significantly diminished its lethal effects ($P < 0.05$; Fig 7C). Consistent with these results, TBAP reduced PCI-32765/bortezomib-induced λH2A.X formation, but did not prevent inactivation of AKT. Similar results were obtained in SUDHL6 cells (Fig 7D), Together, these findings suggest that potentiation of oxidative injury contributes to synergistic interactions between PCI-32765 and bortezomib in DLBCL cells.

DISCUSSION

Evidence of the role of the BCR signalling complex in B-cell transformation (Davis *et al*, 2010) prompted the development of the BTK inhibitor ibrutinib, which in pre-clinical studies has shown impressive activity against both CLL and DLBCL cells (Herman *et al*, 2011;Balbasubramanian *et al*, 2011). The ability of ibrutinib to kill these cells has been linked to the interruption of three survival signalling pathways, e.g., AKT, ERK, and NF-κB, known to be important for the survival of malignant B-cells (Lopez-Guerra & Colomer, 2010;Castillo *et al*, 2012;Wickremasinghe *et al*, 2011). Importantly, early clinical results suggest significant activity of ibrutinib in CLL, DLBCL, and MCL (Harrison, 2012). However, the activity of single agents, including those that inhibit multiple targets, may be limited by redundant signalling pathways, arguing for combination strategies in this setting (Stommel *et al*, 2007). The observations that bortezomib has established or potential activity in MCL (Fisher *et al*, 2006) and DLBCL (Dunleavy *et al*, 2009) respectively, and that each of the pathways interrupted by ibrutinib has been associated with bortezomib resistance (Kim *et al*, 2012;Orlowski *et al*, 2002;Jung *et al*, 2012), make this an attractive candidate for such a combination strategy. Indeed, the results of this study demonstrate that ibrutinib and bortezomib synergistically induce cell death in broad array of DLBCL and MCL cells, and argue that inhibition of multiple ibrutinib targets contributes to this interaction.

Recent evidence indicates that genetic profiling of the NF-κB dependence of DLBCL cells can predict their sensitivity to certain chemotherapeutic agents. For example, ABC-DLBCL cells, which are NF-κB-dependent, are more sensitive than their GC-counterparts to IKK inhibitors (Lam *et al*, 2005). Significantly, patients with ABC-DLBCL, but not those with GC-DLBCL, benefitted from the addition of bortezomib, which has been shown to inactivate NF-κB, to cytotoxic chemotherapy (Dunleavy *et al*, 2009). Analogously, genetic interruption of the BTK pathway inhibited the growth of ABC-DLBCL cells, but not that of GC-DLBCL cells or cells with *CARD11* mutations (Davis *et al*, 2010). In this context, the lack of BCR signalling in GC cells has recently been attributed to high phosphatase activity (Khalil *et al*, 2012). Moreover, initial clinical studies suggest that ibrutinib exhibits superior activity in ABC-DLBCL (Staudt *et al*, 2011). However, it is important to note that combining ibrutinib with bortezomib was equally effective against ABC-DLBCL and GC-DLBCL cells, and that both types exhibited marked inhibition of NF-κB activation in

response to the combination regimen. In addition to this consideration, multiple mechanisms of action of the ibrutinib/bortezomib regimen may account for its activity in both ABC- and GC-DLBCL cells. Importantly, genetic interruption of NF-κB sensitized DLBCL cells to both ibrutinib and bortezomib. These findings are consistent with prior evidence that other inhibitors of the NF-κB pathway (e.g., flavopiridol) (Takada & Aggarwal, 2004) potentiate bortezomib activity in malignant haematopoietic cells in association with increased NF-κB inactivation (Dai *et al*, 2003). Interestingly, whereas a recent report described bortezomib-mediated NF-κB activation in DLBCL cells resulting from autophagosomal IκBα (Jia *et al*, 2012), we observed inactivation, at least at the intervals monitored here. This discrepancy could reflect the possibility that NF-κB modulation by proteasome inhibitors may depend upon their relative effects on autophagosomal versus proteasomal IκBα degradation. In any case, co-administration of ibrutinib resulted in further NF-κB inactivation in both ABC- and GC-DLBCL cells, which may have lowered activity to levels insufficient for cell survival, including in cells not inherently addicted to this pathway.

Co-administration of ibrutinib with bortezomib resulted in the early and pronounced inactivation of AKT as well as multiple downstream AKT targets. BCR-mediated AKT activation is mediated by multiple protein tyrosine kinases, including both SYK and BTK (Craxton *et al*, 1999). AKT activation promotes cell survival through multiple mechanisms, including down-regulation of pro-apoptotic proteins such as BAD and Bim (Datta *et al*, 1997), and activation of NF-κB (Datta *et al*, 1999). Of note, AKT activation status has been shown to be an important determinant of bortezomib sensitivity in transformed cells (Chen *et al*, 2008), including MCL cells (Kim *et al*, 2012). The observation that cells expressing constitutively active (myristolated) AKT were significantly less sensitive to ibrutinib/bortezomib than their control counterparts supports the notion that AKT inactivation plays a significant functional role in cell death induction by this regimen. In contrast, combined exposure of DLBCL cells to ibrutinib/bortezomib failed to induce down-regulation of the MEK1/2/ERK1/2 pathway, which generally exerts a cytoprotective role Notably, the observation that constitutive activation of MEK1/2/ERK1/2 failed to diminish ibrutinib/bortezomib activity argues against a functional role for ERK1/2 inactivation in the activity of this regimen. In contrast to results in DLBCL cells, combined bortezomib/PCI32765 exposure did diminish, although only modestly, ERK1/2 phosphorylation in Granta cells. Whether this action contributed to regimen activity in these cells remains to be determined.

Exposure of DLBCL and MCL cells to minimally toxic concentrations of ibrutinib induced pronounced increases in ROS unaccompanied by evidence of significant DNA damage (e.g., γH2A.X formation). However, co-administration of bortezomib enhanced ROS production further, and led to a striking increase in γH2A.X formation. Induction of ROS has been implicated in bortezomib activity toward malignant epithelial (Ling *et al*, 2003) and haematopoietic cells (Yu *et al*, 2004), but to the best of our knowledge, has not been associated with ibrutinib actions. The latter phenomenon is consistent with evidence that pathways interrupted by ibrutinib, e.g., NF-κB (Dai *et al*, 2005) and AKT (Gao *et al*, 2005;Kim *et al*, 2001), has individually been shown to protect cells from oxidative injury. Furthermore, interruption of AKT is known to disable DNA repair processes (Toulany *et al*, 2006). Thus, co-adminstration of ibrutinib may both increase ROS production in DLBCL and MCL cells while simultaneously potentiating lethal DNA damage by attenuating repair. The ability of antioxidants, such as TBAP, to diminish ibrutinib/bortezomib effects in these cells supports a significant functional role for oxidative injury in synergistic interactions.

Co-administration of ibrutinib and bortezomib synergistically increased cell death in DLBCL and MCL cells resistant to bortezomib. Mechanisms of resistance to proteasome inhibitors may be multifactorial, and include mutations in, or over-expression of proteasome sub-units, increased expression of heat shock proteins, and up-regulation of anti-apoptotic

proteins, such as Bcl-2 or Mcl-1, among others (Mujtaba & Dou, 2011). In addition, increased activation of NF-κB (Jung *et al*, 2012) or AKT (Kim *et al*, 2012) has been described in bortezomib-resistant cells. In the present studies, mechanisms postulated to contribute to synergistic interactions between ibrutinib and bortezomib in parental DLBCL and MCL cells were observed in their bortezomib-resistant counterparts, e.g., inactivation of NF-κB, AKT, and Mcl-1 down-regulation. In this context, Mcl-1 has been implicated in resistance of malignant haematopoietic cells to bortezomib (Hu *et al*, 2012). In addition, recent studies have implicated diminished oxidative injury in resistance of malignant haematopoietic cells (e.g., MCL) to proteasome inhibitors (Weniger *et al*, 2011). Significantly, ibrutinib/bortezomib co-administration promoted ROS generation and sharply increased DNA damage (e.g., γH2A.X formation) in bortezomib-resistant cells, arguing that oxidative injury contributes to the effectiveness of the ibrutinib/bortezomib regimen in the present studies. Finally, it is noteworthy that in contrast to results obtained with other AKT inhibitors (e.g., 2-medroxyestradiol), in which ROS generation was shown to be responsible for AKT inactivation in malignant haematopoietic cells (Gao *et al*, 2005), TBAP failed to prevent PCI-32765/bortezomib-mediated AKT dephosphorylation in DLBCL cells. These findings, as well as the observed protective effects of constitutive AKT activation, suggest that in the present setting, AKT inactivation operates upstream of ROS generation to promote regimen-induced cell death.

The unfolded protein response to ER stress is a dynamic process that may initially serve a protective function but which may ultimately promote cell death (Lin *et al*, 2007). Proteasome inhibitors, such as bortezomib, which prevent protein degradation are well-established inducers of ER stress (Obeng *et al*, 2006). It is noteworthy that co-administration of PCI-32765 with bortezomib induced evidence of this process in both bortezomib-sensitive and –resistant DLBCL cells. Because NF-κB is known to regulate the ER stress response (Xu *et al*, 2005), it is tempting to speculate that the marked reduction in NF-κB activation in cells exposed to both PCI-32765 and bortezomib may have contributed to this event. Additional studies will be required to test this hypothesis. Regardless of the mechanism, the reduced sensitivity of DLBCL cells expressing dominant-negative eIF2α to the PCI-32765/bortezomib regimen suggests that the ER stress response contributes to cell death in this setting.

In summary, the present results suggest that the BTK inhibitor PCI-32765 and the proteasome inhibitor bortezomib interact synergistically in DLBCL and MCL cells, through multiple mechanisms, including induction of ROS and DNA damage, down-regulation of anti-apoptotic proteins (e.g., Mcl-1, Bcl-xL), inactivation of the AKT and NF-κB pathways, and induction of ER stress. Notably, in contrast to preclinical results involving BTK inhibition alone (Davis *et al*, 2010), this strategy is equally effective in ABC- and GC-subtypes of DLBCL, as well as in bortezomib-resistant cells. In view of emerging or established evidence of activity of these agents in DLBCL and MCL, further exploration of this strategy in the *in vivo* setting appears justified, and is currently underway.

Supplementary Material

Refer to Web version on PubMed Central for supplementary material.

Acknowledgments

This work was supported by Lymphoma SPORE award 1P50 CA130805. CA63753, CA93738, and CA100866 from the National Institutes of Health; award R6059-06 from the Leukemia and Lymphoma Society of America, the Multiple Myeloma Research Foundation, Myeloma Spore (P50CA142509) and the V Foundation.

References

Adams J, Palombella VJ, Sausville EA, Johnson J, Destree A, Lazarus DD, Maas J, Pien CS, Prakash S, Elliott PJ. Proteasome inhibitors: a novel class of potent and effective antitumor agents. Cancer Res. 1999; 59:2615–2622. [PubMed: 10363983]

An B, Goldfarb RH, Siman R, Dou QP. Novel dipeptidyl proteasome inhibitors overcome Bcl-2 protective function and selectively accumulate the cyclin-dependent kinase inhibitor p27 and induce apoptosis in transformed, but not normal, human fibroblasts. Cell Death.Differ. 1998; 5:1062–1075. [PubMed: 9894613]

Balbasubramanian S, Crowley S, Sirisiwad M, Thiemann P, Chen J, Buggy J. The Bruton's Tyrosine Kinase (BTK) Inhibitor PCI-32765 Inhibits Growth of ABC DLBCL Tumors In Vivo and in Vitro by Preventing Activation of Pro-Survival NF-{kappa}B pathways. Blood (ASH annual Meeting Abstracts). 2011; 117:4969.

Bea S, Zettl A, Wright G, Salaverria I, Jehn P, Moreno V, Burek C, Ott G, Puig X, Yang L, Lopez-Guillermo A, Chan WC, Greiner TC, Weisenburger DD, Armitage JO, Gascoyne RD, Connors JM, Grogan TM, Braziel R, Fisher RI, Smeland EB, Kvaloy S, Holte H, Delabie J, Simon R, Powell J, Wilson WH, Jaffe ES, Montserrat E, Muller-Hermelink HK, Staudt LM, Campo E, Rosenwald A. Diffuse large B-cell lymphoma subgroups have distinct genetic profiles that influence tumor biology and improve gene-expression-based survival prediction. Blood. 2005; 106:3183–3190. [PubMed: 16046532]

Bedford L, Lowe J, Dick LR, Mayer RJ, Brownell JE. Ubiquitin-like protein conjugation and the ubiquitin-proteasome system as drug targets. Nat.Rev.Drug Discov. 2011; 10:29–46. [PubMed: 21151032]

Castillo JJ, Furman M, Winer ES. CAL-101: a phosphatidylinositol-3-kinase p110-delta inhibitor for the treatment of lymphoid malignancies. Expert.Opin.Investig.Drugs. 2012; 21:15–22.

Celeste A, Petersen S, Romanienko PJ, Fernandez-Capetillo O, Chen HT, Sedelnikova OA, Reina-San-Martin B, Coppola V, Meffre E, Difilippantonio MJ, Redon C, Pilch DR, Olaru A, Eckhaus M, Camerini-Otero RD, Tessarollo L, Livak F, Manova K, Bonner WM, Nussenzweig MC, Nussenzweig A. Genomic instability in mice lacking histone H2AX. Science. 2002; 296:922–927. [PubMed: 11934988]

Chen KF, Yeh PY, Yeh KH, Lu YS, Huang SY, Cheng AL. Down-regulation of phospho-Akt is a major molecular determinant of bortezomib-induced apoptosis in hepatocellular carcinoma cells. Cancer Res. 2008; 68:6698–6707. [PubMed: 18701494]

Chou TC, Talalay P. Quantitative analysis of dose-effect relationships: the combined effects of multiple drugs or enzyme inhibitors. Adv.Enzyme Regul. 1984; 22:27–55. [PubMed: 6382953]

Compagno M, Lim WK, Grunn A, Nandula SV, Brahmachary M, Shen Q, Bertoni F, Ponzoni M, Scandurra M, Califano A, Bhagat G, Chadburn A, Dalla-Favera R, Pasqualucci L. Mutations of multiple genes cause deregulation of NF-kappaB in diffuse large B-cell lymphoma. Nature. 2009; 459:717–721. [PubMed: 19412164]

Craxton A, Jiang A, Kurosaki T, Clark EA. Syk and Bruton's tyrosine kinase are required for B cell antigen receptor-mediated activation of the kinase Akt. J.Biol.Chem. 1999; 274:30644–30650. [PubMed: 10521450]

Dai Y, Rahmani M, Grant S. Proteasome inhibitors potentiate leukemic cell apoptosis induced by the cyclin-dependent kinase inhibitor flavopiridol through a SAPK/JNK- and NF-kappaB-dependent process. Oncogene. 2003; 22:7108–7122. [PubMed: 14562039]

Dai Y, Rahmani M, Dent P, Grant S. Blockade of histone deacetylase inhibitor-induced RelA/p65 acetylation and NF-kappaB activation potentiates apoptosis in leukemia cells through a process mediated by oxidative damage, XIAP downregulation, and c-Jun N-terminal kinase 1 activation. Mol.Cell Biol. 2005; 25:5429–5444. [PubMed: 15964800]

Dasmahapatra G, Lembersky D, Rahmani M, Kramer L, Friedberg J, Fisher RI, Dent P, Grant S. Bcl-2 antagonists interact synergistically with bortezomib in DLBCL cells in association with JNK activation and induction of ER stress. Cancer Biol.Ther. 2009; 8:808–819. [PubMed: 19270531]

Dasmahapatra G, Lembersky D, Kramer L, Fisher RI, Friedberg J, Dent P, Grant S. The pan-HDAC inhibitor vorinostat potentiates the activity of the proteasome inhibitor carfilzomib in human DLBCL cells in vitro and in vivo. Blood. 2010; 115:4478–4487. [PubMed: 20233973]

Dasmahapatra G, Lembersky D, Son MP, Attkisson E, Dent P, Fisher RI, Friedberg JW, Grant S. Carfilzomib interacts synergistically with histone deacetylase inhibitors in mantle cell lymphoma cells in vitro and in vivo. Mol.Cancer Ther. 2011; 10:1686–1697. [PubMed: 21750224]

Dasmahapatra G, Lembersky D, Son MP, Patel H, Peterson D, Attkisson E, Fisher RI, Friedberg JW, Dent P, Grant S. Obatoclax interacts synergistically with the irreversible proteasome inhibitor carfilzomib in GC- and ABC-DLBCL cells in vitro and in vivo. Mol.Cancer Ther. 2012; 11:1122–1132. [PubMed: 22411899]

Datta SR, Dudek H, Tao X, Masters S, Fu H, Gotoh Y, Greenberg ME. Akt phosphorylation of BAD couples survival signals to the cell-intrinsic death machinery. Cell. 1997; 91:231–241. [PubMed: 9346240]

Datta SR, Brunet A, Greenberg ME. Cellular survival: a play in three Akts. Genes Dev. 1999; 13:2905–2927. [PubMed: 10579998]

Davis RE, Ngo VN, Lenz G, Tolar P, Young RM, Romesser PB, Kohlhammer H, Lamy L, Zhao H, Yang Y, Xu W, Shaffer AL, Wright G, Xiao W, Powell J, Jiang JK, Thomas CJ, Rosenwald A, Ott G, Muller-Hermelink HK, Gascoyne RD, Connors JM, Johnson NA, Rimsza LM, Campo E, Jaffe ES, Wilson WH, Delabie J, Smeland EB, Fisher RI, Braziel RM, Tubbs RR, Cook JR, Weisenburger DD, Chan WC, Pierce SK, Staudt LM. Chronic active B-cell-receptor signalling in diffuse large B-cell lymphoma. Nature. 2010; 463:88–92. [PubMed: 20054396]

Dunleavy K, Pittaluga S, Czuczman MS, Dave SS, Wright G, Grant N, Shovlin M, Jaffe ES, Janik JE, Staudt LM, Wilson WH. Differential efficacy of bortezomib plus chemotherapy within molecular subtypes of diffuse large B-cell lymphoma. Blood. 2009; 113:6069–6076. [PubMed: 19380866]

Fisher RI, Bernstein SH, Kahl BS, Djulbegovic B, Robertson MJ, de VS, Epner E, Krishnan A, Leonard JP, Lonial S, Stadtmauer EA, O'Connor OA, Shi H, Boral AL, Goy A. Multicenter phase II study of bortezomib in patients with relapsed or refractory mantle cell lymphoma. J.Clin.Oncol. 2006; 24:4867–4874. [PubMed: 17001068]

Gao N, Rahmani M, Dent P, Grant S. 2-Methoxyestradiol-induced apoptosis in human leukemia cells proceeds through a reactive oxygen species and Akt-dependent process. Oncogene. 2005; 24:3797–3809. [PubMed: 15782127]

Goy A, Younes A, McLaughlin P, Pro B, Romaguera JE, Hagemeister F, Fayad L, Dang NH, Samaniego F, Wang M, Broglio K, Samuels B, Gilles F, Sarris AH, Hart S, Trehu E, Schenkein D, Cabanillas F, Rodriguez AM. Phase II study of proteasome inhibitor bortezomib in relapsed or refractory B-cell non-Hodgkin's lymphoma. J.Clin.Oncol. 2005; 23:667–675. [PubMed: 15613697]

Harrison C. Trial watch: BTK inhibitor shows positive results in B cell malignancies. Nat.Rev.Drug Discov. 2012; 11:96. [PubMed: 22262035]

Herman SE, Gordon AL, Hertlein E, Ramanunni A, Zhang X, Jaglowski S, Flynn J, Jones J, Blum KA, Buggy JJ, Hamdy A, Johnson AJ, Byrd JC. Bruton tyrosine kinase represents a promising therapeutic target for treatment of chronic lymphocytic leukemia and is effectively targeted by PCI-32765. Blood. 2011; 117:6287–6296. [PubMed: 21422473]

Hideshima T, Ikeda H, Chauhan D, Okawa Y, Raje N, Podar K, Mitsiades C, Munshi NC, Richardson PG, Carrasco RD, Anderson KC. Bortezomib induces canonical nuclear factor-kappaB activation in multiple myeloma cells. Blood. 2009; 114:1046–1052. [PubMed: 19436050]

Honigberg LA, Smith AM, Sirisawad M, Verner E, Loury D, Chang B, Li S, Pan Z, Thamm DH, Miller RA, Buggy JJ. The Bruton tyrosine kinase inhibitor PCI-32765 blocks B-cell activation and is efficacious in models of autoimmune disease and B-cell malignancy. Proc.Natl.Acad.Sci.U.S.A. 2010; 107:13075–13080. [PubMed: 20615965]

Hu J, Dang N, Menu E, De BE, Xu D, Van CB, Van VE, Vanderkerken K. Activation of ATF4 mediates the unwanted Mcl-1 accumulation by proteasome inhibition. Blood. 2012; 119:826–37. [PubMed: 22128141]

Hussain A, Yu L, Faryal R, Mohammad DK, Mohamed AJ, Smith CI. TEC family kinases in health and disease - loss-of-function of BTK and ITK and the gain-of-function fusions ITK-SYK and BTK-SYK. FEBS J. 2011; 278:2001–2010. [PubMed: 21518255]

Ikeda H, Hideshima T, Fulciniti M, Perrone G, Miura N, Yasui H, Okawa Y, Kiziltepe T, Santo L, Vallet S, Cristea D, Calabrese E, Gorgun G, Raje NS, Richardson P, Munshi NC, Lannutti BJ, Puri

KD, Giese NA, Anderson KC. PI3K/p110{delta} is a novel therapeutic target in multiple myeloma. Blood. 2010; 116:1460–1468. [PubMed: 20505158]

Jia L, Gopinathan G, Sukumar JT, Gribben JG. Blocking autophagy prevents bortezomib-induced NF-kappaB activation by reducing I-kappaBalpha degradation in lymphoma cells. PLoS.One. 2012; 7:e32584. [PubMed: 22393418]

Jung HJ, Chen Z, Fayad L, Wang M, Romaguera J, Kwak LW, McCarty N. Bortezomib-resistant nuclear factor kappaB expression in stem-like cells in mantle cell lymphoma. Exp.Hematol. 2012; 40:107–118. [PubMed: 22024108]

Khalil AM, Cambier JC, Shlomchik MJ. B cell receptor signal transduction in the GC is short-circuited by high phosphatase activity. Science. 2012; 336:1178–1181. [PubMed: 22555432]

Kim A, Park S, Lee JE, Jang WS, Lee SJ, Kang HJ, Lee SS. The dual PI3K and mTOR inhibitor NVP-BEZ235 exhibits anti-proliferative activity and overcomes bortezomib resistance in mantle cell lymphoma cells. Leuk.Res. 2012; 36:912–920. [PubMed: 22560334]

Kim AH, Khursigara G, Sun X, Franke TF, Chao MV. Akt phosphorylates and negatively regulates apoptosis signal-regulating kinase 1. Mol.Cell Biol. 2001; 21:893–901. [PubMed: 11154276]

Lam LT, Davis RE, Pierce J, Hepperle M, Xu Y, Hottelet M, Nong Y, Wen D, Adams J, Dang L, Staudt LM. Small molecule inhibitors of IkappaB kinase are selectively toxic for subgroups of diffuse large B-cell lymphoma defined by gene expression profiling. Clin.Cancer Res. 2005; 11:28–40. [PubMed: 15671525]

Lin JH, Li H, Yasumura D, Cohen HR, Zhang C, Panning B, Shokat KM, Lavail MM, Walter P. IRE1 signaling affects cell fate during the unfolded protein response. Science. 2007; 318:944–949. [PubMed: 17991856]

Ling YH, Liebes L, Zou Y, Perez-Soler R. Reactive oxygen species generation and mitochondrial dysfunction in the apoptotic response to Bortezomib, a novel proteasome inhibitor, in human H460 non-small cell lung cancer cells. J.Biol.Chem. 2003; 278:33714–33723. [PubMed: 12821677]

Lopez-Guerra M, Colomer D. NF-kappaB as a therapeutic target in chronic lymphocytic leukemia. Expert.Opin.Ther.Targets. 2010; 14:275–288. [PubMed: 20148715]

Mohamed AJ, Yu L, Backesjo CM, Vargas L, Faryal R, Aints A, Christensson B, Berglof A, Vihinen M, Nore BF, Smith CI. Bruton's tyrosine kinase (Btk): function, regulation, and transformation with special emphasis on the PH domain. Immunol.Rev. 2009; 228:58–73. [PubMed: 19290921]

Mujtaba T, Dou QP. Advances in the understanding of mechanisms and therapeutic use of bortezomib. Discov.Med. 2011; 12:471–480. [PubMed: 22204764]

Nencioni A, Grunebach F, Patrone F, Ballestrero A, Brossart P. Proteasome inhibitors: antitumor effects and beyond. Leukemia. 2007; 21:30–36. [PubMed: 17096016]

O'Brien S, Buger JA, Blum KA, Furman RR, Coutre SE, Sharman J, Flinn IW, Grant B, Heerema NA, Johnson AJ, Navarro T, Holmgren E, Hedrick E, Byrd JC. The Bruton's Tyrosine Kinase (BTK) Inhibitor PCI-32765 Induces Durable Responses in Relapsed or Refractory (R/R) Chronic Lymphocytic Leukemia/Small Lymphocytic Lymphoma (CLL/SLL): Follow-up of a Phase Ib/II Study. Blood (ASH annual Meeting Abstracts). 2011; 118:983.

Obeng EA, Carlson LM, Gutman DM, Harrington WJ Jr. Lee KP, Boise LH. Proteasome inhibitors induce a terminal unfolded protein response in multiple myeloma cells. Blood. 2006; 107:4907–4916. [PubMed: 16507771]

Orlowski RZ, Small GW, Shi YY. Evidence that inhibition of p44/42 mitogen-activated protein kinase signaling is a factor in proteasome inhibitor-mediated apoptosis. J.Biol.Chem. 2002; 277:27864–27871. [PubMed: 12023956]

Rahmani M, Davis E, Crabtree T, Habibi J, Nguyen T, Dent P, Grant S. The kinase inhibitor sorafenib induces cell death through a process involving induction of ER stress. Molecular and Cellular Biology. 2007; 27:5499–5413. [PubMed: 17548474]

Rawlings DJ, Scharenberg AM, Park H, Wahl MI, Lin S, Kato RM, Fluckiger AC, Witte ON, Kinet JP. Activation of BTK by a phosphorylation mechanism initiated by SRC family kinases. Science. 1996; 271:822–825. [PubMed: 8629002]

Richardson PG, Mitsiades C, Hideshima T, Anderson KC. Bortezomib: proteasome inhibition as an effective anticancer therapy. Annu.Rev.Med. 2006; 57:33–47. [PubMed: 16409135]

Staudt L, Dunleavy K, Buggy J, Hedrick E, Lucas N, Pittaluga S, Javar S, Schmidt R, Williams M, Lih J, Jaffe E, Wilson W. The Bruton's Tyrosine Kinase (Btk) Inhibitor PCI-32765 Modulates Chronic Active BCR Signaling and Induces Tumor Regression in Relapsed/Refractory ABC DLBCL. Blood (ASH annual Meeting Abstracts). 2011; 118:2716.

Staudt LM, Dave S. The biology of human lymphoid malignancies revealed by gene expression profiling. Adv.Immunol. 2005; 87:163–208. [PubMed: 16102574]

Stommel JM, Kimmelman AC, Ying H, Nabioullin R, Ponugoti AH, Wiedemeyer R, Stegh AH, Bradner JE, Ligon KL, Brennan C, Chin L, DePinho RA. Coactivation of receptor tyrosine kinases affects the response of tumor cells to targeted therapies. Science. 2007; 318:287–290. [PubMed: 17872411]

Takada Y, Aggarwal BB. Flavopiridol inhibits NF-kappaB activation induced by various carcinogens and inflammatory agents through inhibition of IkappaBalpha kinase and p65 phosphorylation: abrogation of cyclin D1, cyclooxygenase-2, and matrix metalloprotease-9. J.Biol.Chem. 2004; 279:4750–4759. [PubMed: 14630924]

Teske BF, Wek SA, Bunpo P, Cundiff JK, McClintick JN, Anthony TG, Wek RC. The eIF2 kinase PERK and the integrated stress response facilitate activation of ATF6 during endoplasmic reticulum stress. Mol.Biol.Cell. 2011; 22:4390–4405. [PubMed: 21917591]

Toulany M, Kasten-Pisula U, Brammer I, Wang S, Chen J, Dittmann K, Baumann M, Dikomey E, Rodemann HP. Blockage of epidermal growth factor receptor-phosphatidylinositol 3-kinase-AKT signaling increases radiosensitivity of K-RAS mutated human tumor cells in vitro by affecting DNA repair. Clin.Cancer Res. 2006; 12:4119–4126. [PubMed: 16818713]

Wang L, Martin P, Blum K, Kahl B, Maeda L, Advani R, Williams M, Rule S, Rodriguez S, Pang C, Hedrick E, Goy A. The Bruton's tyrosine kinase inhibitor PCI-32765 is highly active as single-agent therapy in previously treated mantle cell lymphoma: Preliminary results of a phase II trial. Blood (ASH annual Meeting Abstracts). 2011; 118:442.

Weniger MA, Rizzatti EG, Perez-Galan P, Liu D, Wang Q, Munson PJ, Raghavachari N, White T, Tweito MM, Dunleavy K, Ye Y, Wilson WH, Wiestner A. Treatment-induced oxidative stress and cellular antioxidant capacity determine response to bortezomib in mantle cell lymphoma. Clin.Cancer Res. 2011; 17:5101–5112. [PubMed: 21712452]

Wickremasinghe RG, Prentice AG, Steele AJ. Aberrantly activated anti-apoptotic signalling mechanisms in chronic lymphocytic leukaemia cells: clues to the identification of novel therapeutic targets. Br.J.Haematol. 2011; 153:545–556. [PubMed: 21501136]

Williams ME, Connors JM, Dreyling MH, Gascoyne RD, Kahl BS, Leonard JP, Press OW, Wilson WH. Mantle cell lymphoma: report of the 2010 Mantle Cell Lymphoma Consortium Workshop. Leuk.Lymphoma. 2011; 52:24–33. [PubMed: 21133727]

Xu C, Bailly-Maitre B, Reed JC. Endoplasmic reticulum stress: cell life and death decisions. J.Clin.Invest. 2005; 115:2656–2664. [PubMed: 16200199]

Yeramian A, Sorolla A, Velasco A, Santacana M, Dolcet X, Valls J, Abal L, Moreno S, Egido R, Casanova JM, Puig S, Vilella R, Llombart-Cussac A, Matias-Guiu X, Marti RM. Inhibition of activated receptor tyrosine kinases by Sunitinib induces growth arrest and sensitizes melanoma cells to Bortezomib by blocking Akt pathway. Int.J.Cancer. 2012; 130:967–978. [PubMed: 21445974]

Yu C, Rahmani M, Dent P, Grant S. The hierarchical relationship between MAPK signaling and ROS generation in human leukemia cells undergoing apoptosis in response to the proteasome inhibitor Bortezomib. Exp.Cell Res. 2004; 295:555–566. [PubMed: 15093752]

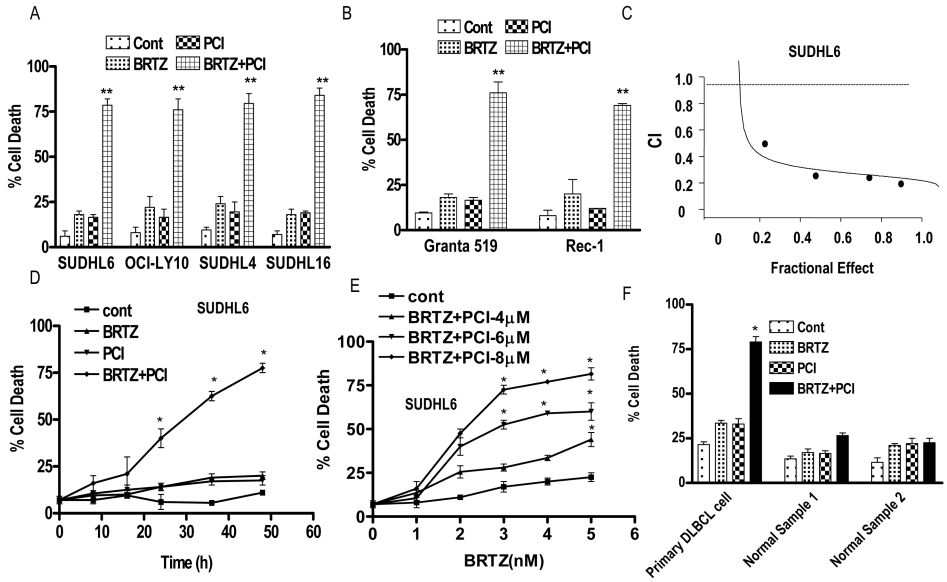

Figure 1. PCI-32765 and bortezomib interact synergistically in ABC or GC-DLBCL cells and MCL cells but not in normal cells

(A-B) Cells were treated with minimally toxic concentrations of bortezomib (SUDHL6 3 nM, OCI-LY10 8 nM, SUDHL4 5 nM, SUDHL16 2.5 nM, Granta 519 5 nM, Rec-1 15 nM) in the presence or absence of PCI (SUDHL6 7.5 μM, OCI-LY10 6 μM, SUDHL4 7.5 μM, SUDHL16 5.0 μM, Granta 519 7.5 μM, Rec-1 7.5 μM) for 48 h, after which cell death was monitored by 7-AAD staining and flow cytometry (C) Fractional Effect values were determined by comparing results obtained for untreated controls and treated cells following 48-h exposure to agents administered at a fixed ratio (bortezomib:PCI, 1:2500), after which Median Dose Effect analysis was employed to characterize the nature of the interaction. Combination Index (CI) values less than 1.0 denote a synergistic interaction. (D) SUDHL6 cells were treated with bortezomib 3.0 nM ± PCI 7.5 μM for different time intervals, after which cell death was monitored by flow cytometry and 7-AAD staining. (E) SUDHL6 cells were treated with varying PCI (4-8 μM) concentrations in the presence or absence of fixed concentrations of bortezomib (1.0 or 5.0 nM) for 48 h, after which cell death was monitored by flow cytometry and 7-AAD staining (F) Primary human DLBCL (GC subtype) mononuclear cells (96% purity) were isolated as described in Methods and re-suspended in medium containing 10% fetal calf serum at a cell density of 0.75×10^6/ml cells. They were then treated with bortezomib (4 nM) ± PCI32765 (6.0 μM) for 10 h. $CD34^+$ cells were collected from the bone marrow, isolated by an immunomagnetic bead separation technique as described in Methods, and exposed to bortezomib ± PCI as indicated for 48 h. Cell death was monitored by Annexin V/propidium iodide staining. For all studies, values represent the means for 3 experiments performed in triplicate ± S.D. For A-B ** = significantly more than values obtained for bortezomib or PCI treatment alone < 0.02. D-F, * = significantly greater than values obtained for bortezomib or PCI treatment alone in SUDHL6 cells or primary DLBCL cells; $P < 0.05$. Cont, control; BRTZ, bortezomib; PCI, PCI-32765.

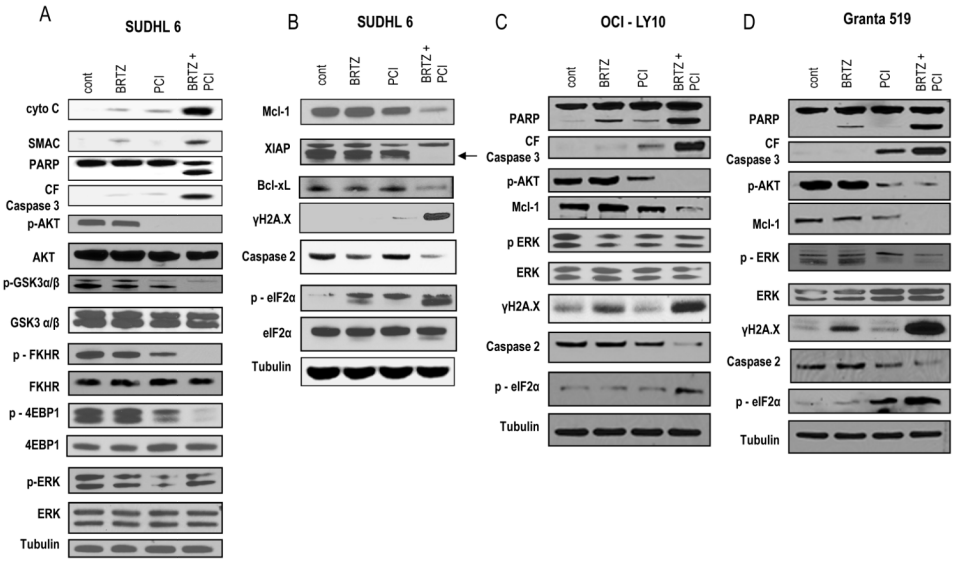

Figure 2. Co-exposure of DLBCL or MCL cells to PCI-32765 and bortezomib leads to modulation of multiple survival and stress-related pathways

(A) SUDHL6 cells were treated for 24 h with bortezomib (3.0 nM) ± PCI (7.5 μM). (B) OCI-LY10 cells were treated for 24 h with bortezomib (8.0 nM) ± PCI (6.0 μM). (C) Granta cells were treated for 24 h with bortezomib (5.0 nM) ± PCI (7.5 μM). (A-C) Expression of the indicated proteins was determined by Western blotting using indicated antibodies. Each lane was loaded with 20 μg of protein; blots were stripped and re-probed with antibodies to tubulin to ensure equivalent loading and transfer. Results are representative of three independent experiments. cont, control; BRTZ, bortezomib; PCI, PCI-32765.

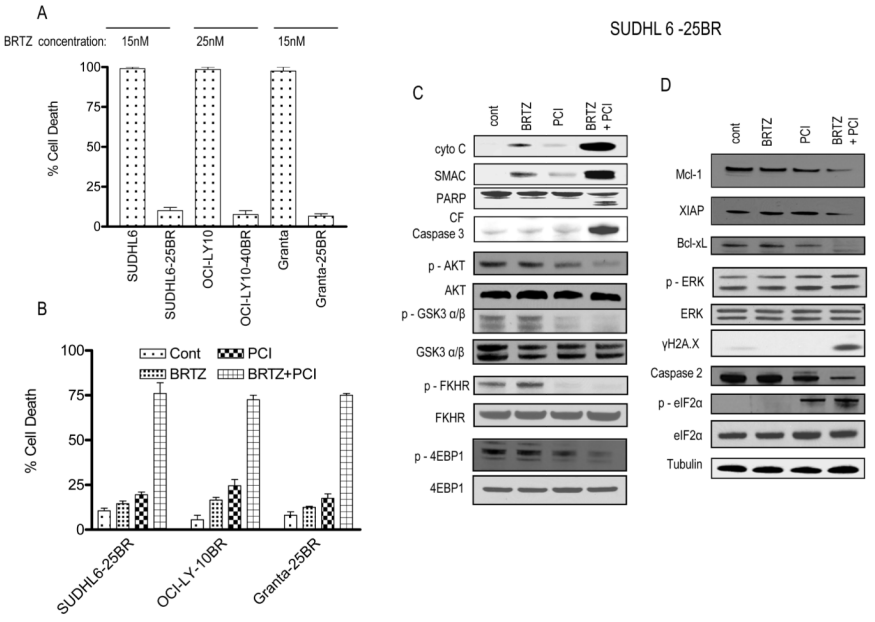

Figure 3. PCI-32765 and bortezomib interact synergistically in bortezomib-resistant DLBCL and MCL cells

(A) Bortezomib-resistant SUDHL6-25BR, OCI-LY10-40BR, Granta-25BR cells and their parental counterparts were treated for 48 h with the indicated concentration of bortezomib, after which cell death was monitored by 7-AAD staining and flow cytometry. Results represent the means ± standard deviation for 3 separate experiments performed in triplicate. (B) SUDHL6-25BR, OCI-LY10-40BR, Granta-25BR cells were treated with minimally toxic concentrations of bortezomib and PCI. Concentrations were as follows: SUDHL6-25BR - bortezomib (15 nM) ± PCI (7.5 μM), OCI-LY10-40BR - bortezomib (25 nM) ± PCI (6.0 μM), Granta – 25BR - bortezomib (15 nM) ± PCI (7.5 μM). Cell death was monitored by 7-AAD after 48 h, as described above in A. (C-D) SUDHL6-25BR cells were exposed for 24 h to bortezomib and PCI as in (B), after which Western blot analysis was performed with the indicated antibodies. cont, control; BRTZ, bortezomib; PCI, PCI-32765.

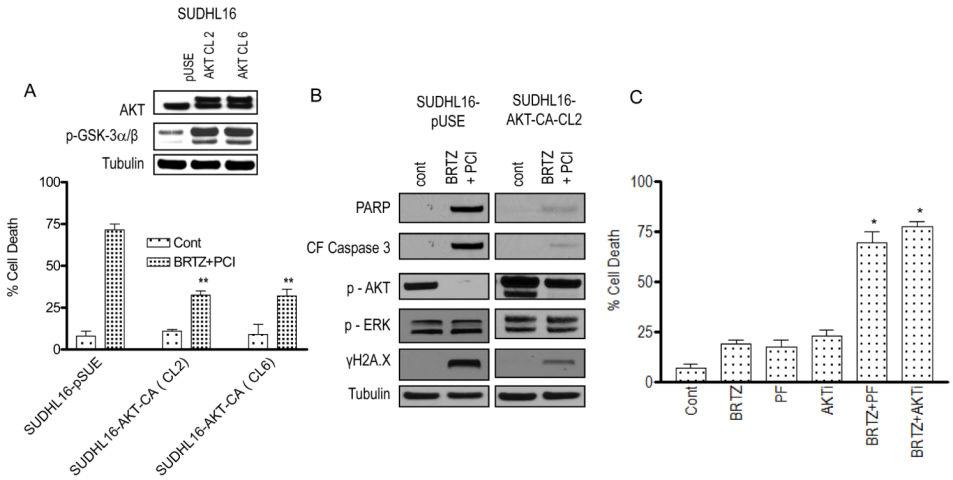

Figure 4. AKT inactivation plays a significant functional role in PCI-32765/bortezomib synergism

SUDHL16 cells were stably transfected with constitutively active (myristolated) AKT constructs (AKT cl.2 and 6) or empty vector (pUSE), and exposed for 48 h to bortezomib (3.0 nM) ± PCI (5.0 μM), after which cell death was monitored by 7-AAD staining and flow cytometry. Results represent the means ± standard deviation (SD) for 3 separate experiments performed in triplicate. *Inset*: Western blots showing expression of AKT and p-GSK-3α/β in empty vector control and AKT clones. (B) Cells were treated as described above in (A) for 24 h, after which Western blot analysis was performed to monitor expression of the indicated proteins. Each lane was loaded with 20 μg of protein; blots were stripped and re-probed with antibodies to tubulin to ensure equivalent loading and transfer. Results are representative of three independent experiments. (C) SUDHL6 cells were treated for 48 h with bortezomib (3 nM) ± perifosine (PF: 2.5 μM) or AKTi (500 nM) after which cell death was monitored by 7-AAD staining and flow cytometry. Results represent the means ± SD for 3 separate experiments performed in triplicate. For A, ** = significantly less than values obtained for bortezomib + PCI treatment in SUDHL16 cells expressing pUSE cells; $P < 0.02$. C, * = significantly more than values obtained for bortezomib, perifosine or AKTi treatment alone in SUDHL6 cell; $P < 0.05$. cont, control; BRTZ, bortezomib; PCI, PCI-32765.

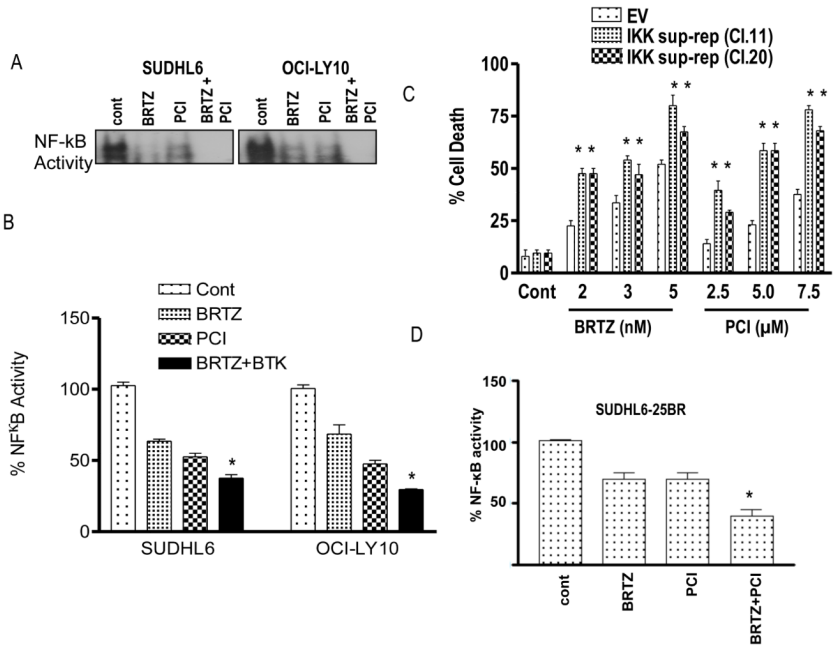

Figure 5. Evidence for the contribution of inactivation of NF-κB to PCI-32765/bortezomib synergism

(A) SUDHL 6 and OCI-LY10 - DLBCL cells were treated with bortezomib (3.0-8.0 nM) ± PCI (6-7.5 μM) and for 24 h. Nuclear proteins were extracted using a nuclear extract kit (Active Motif) and then subjected to electrophoretic mobility shift assay (EMSA) gel shift assays to assess NF-κB DNA binding as described in Methods. (B) Using the same nuclear proteins, NF-κB activity was determined using an enzyme-linked immunosorbent assay (ELISA) TransAM NF-κB p65 Transcription Factor Assay Kit (Active Motif), as described in Methods. (C) SUDHL16-IKK super repressor cell (sup-rep) with empty vector control was treated with the indicated concentration of either bortezomib or PCI alone for 48 h and cell death was measured by 7AAD staining. (D) SUDHL 6-25BR cells were treated with bortezomib (15 nM) ± PCI (7.5 μM) for 24 h. Nuclear proteins were extracted using a nuclear extract kit (Active Motif) and NF-κB activity was determined using an ELISA TransAM NF-κB p65 Transcription Factor Assay Kit (Active Motif), as described in Methods. Values represent the means ± standard deviation of triplicate determinations for 3 separate experiments. For B & D * = significantly less than values for bortezomib or PCI alone; $P < 0.05$, For C ** = significantly greater than values for bortezomib or PCI alone than empty vector control; $P < 0.05$. cont, control; BRTZ, bortezomib; PCI, PCI-32765.

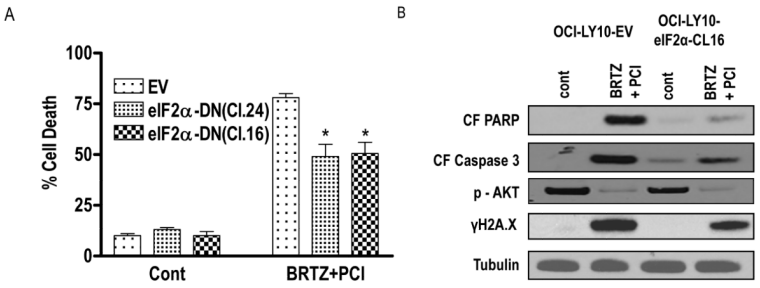

Figure 6. Role of ER stress in PCI-32765/bortezomib activity in DLBCL cells

(A) SUDHL16 cells stably transfected with an eIF2α-DN (CL.24 and Cl.16) or an empty vector (pcDNA3.1) construct were incubated with 2.5 nM bortezomib + 5.0 μM PCI. After 36-h of drug exposure, cell death was monitored by 7-AAD staining and flow cytometry. Values represent the means ± standard deviation for triplicate determinations for 3 separate experiments. (B) Following 16-h of drug exposure to SUDHL16-eIF2α cells and empty vector controls cells as described in (A) above, Western blot analysis was employed to monitor protein expression using the indicated antibodies. Blots were stripped and re-probed with anti-tubilin antibodies to ensure equal loading and transfer of protein (20 μg each lane). For A* = significantly less than values for control cells; $P < 0.05$. Two additional studies yielded equivalent results. cont, control; BRTZ, bortezomib; PCI, PCI-32765.

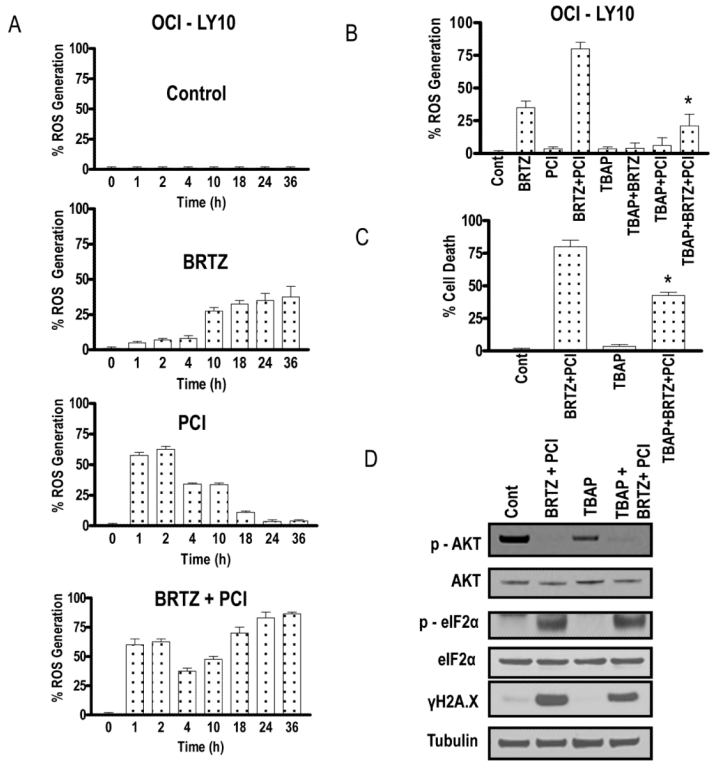

Figure 7. Combined exposure to PCI-32765 and bortezomib leads to oxidative injury-mediated cell death in DLBCL cells

(A) OCI-LY10 cells were treated with bortezomib (8.0 nM) ± PCI (6.0 μM) as above after which reactive oxygen species (ROS) generation was monitored at the indicated intervals (B) OCI-LY10 cells were treated with bortezomib (8.0 nM) ± PCI-6.0 μM (± pre-treatment with 400 μM TBAP for 3 h) for 24 h after which ROS generation was monitored as described in Methods. (C) After treatment as in (B) above for 48 h, cell death was monitored by 7AAD staining (D). Values represent the means ± standard deviation for triplicate determinations for 3 separate experiments. Following 24-h of drug exposure as in (C) above, expression of the indicated proteins was monitored by Western blotting. Blots were stripped and re-probed with anti-tubilin antibodies to ensure equal loading and transfer of protein (20 μg each lane). For B and C, * = significantly different from values for combination treatment without TBAP pretreatment controls, $P < 0.05$. cont, control; BRTZ, bortezomib; PCI, PCI-32765.